



High-z galaxies behind the lensing cluster A2667

N. Laporte, R. Pelló, D. Schaerer, J. Richard, F. Boone, J.-P. Kneib, E. Egami

► To cite this version:

N. Laporte, R. Pelló, D. Schaerer, J. Richard, F. Boone, et al.. High-z galaxies behind the lensing cluster A2667. Annual meeting of the French Society of Astronomy and Astrophysics, 2011, France. pp.141-145. hal-00660206

HAL Id: hal-00660206

<https://hal.science/hal-00660206>

Submitted on 16 Jan 2012

HAL is a multi-disciplinary open access archive for the deposit and dissemination of scientific research documents, whether they are published or not. The documents may come from teaching and research institutions in France or abroad, or from public or private research centers.

L'archive ouverte pluridisciplinaire **HAL**, est destinée au dépôt et à la diffusion de documents scientifiques de niveau recherche, publiés ou non, émanant des établissements d'enseignement et de recherche français ou étrangers, des laboratoires publics ou privés.

HIGH- z GALAXIES BEHIND THE LENSING CLUSTER A2667

N. Laporte¹, R. Pelló¹, D. Schaerer², J. Richard³, F. Boone¹, J.-P. Kneib⁴ and E. Egami⁵

Abstract. We have conducted a survey aimed at identifying a sample of $z \sim 7$ -10 candidates accessible to detailed spectroscopic studies. The deep survey on A2667 covers a large field of view with HAWK-I and FORS2 at ESO/VLT between 0.8 and $2.5\mu\text{m}$ (typical depth $m(\text{AB})=27.5$ at 3σ). 13 sources were identified based on the Lyman Break technique, namely 1 J -drop, 8 Y -drops and 4 z -drops over the $\sim 45 \text{ arcmin}^2$ field of view. Optical and near-IR data were combined with Spitzer and Hubble Space Telescope data, when available, in order to determine photometric redshifts. Although the best-fit is always obtained for a high- z solution, this sample shows a relatively high contamination level from extreme mid- z interlopers which may also be present in other surveys. This is demonstrated by the recent detection of two candidates by Herschel and LABOCA, making the high- z identification unlikely. Waiting for a complete spectroscopic follow up, we have used different criteria to account for this contamination and to derive new constraints on the bright end of the UV LF from $z \sim 7$ to 9, using a MC approach based on the redshift probability distributions. Our results are consistent with a significant evolution in the density of bright galaxies beyond $z \sim 8$, whereas no clear evolution is observed between $z \sim 7$ and 8.

Keywords: gravitational lensing: strong, galaxies: high-redshift, dark ages, reionization, first stars

1 Introduction

Understanding the formation of the first luminous sources in the Universe is one of the most important goal in modern astrophysics. Since few years, considerable advances have been made in the search for and study of the first galaxies, by pushing the farthest candidates at $z \sim 10$ (Bouwens et al. 2011). At the same time, the number of confirmed galaxies at $z \geq 6.0$, taking benefit from the use of the new instruments, as VIMOS@Keck or X-Shooter@VLT (Richard et al. 2011), has greatly increased. We have recently published the first results on the search for high- z galaxies around the lensing cluster A2667 (Laporte et al. 2011, hereafter paper 1) using the Lyman Break Technique (Steidel et al. 1995) and the lensing cluster as a gravitational telescope (Zwicky 1937). In this paper we briefly present the main results of the search for $z \geq 6.5$ sources behind A2667, and then focus on the determination of their Luminosity Function (hereafter LF) and its evolution. In the following, we use the concordance cosmology with $\Omega_\Lambda=0.7$, $\Omega_M=0.3$ and $H_0=70\text{km.s}^{-1}.\text{Mpc}^{-1}$.

2 High- z sample selection

2.1 Observational data

Our project is based on the photometric pre-selection of candidates using deep optical and near-IR images taken with HAWK-I (filters Y , J , H and Ks) and FORS2 (I and z bands) on the VLT combined with Spitzer data (3.6, 4.5, 5.8, 8.0 and $24 \mu\text{m}$) when available. The reader is invited to refer to paper 1 for a complete description of images properties and data processing.

¹ IRAP, 14 Avenue Edouard Belin, 31400 Toulouse & CNRS; IRAP; 14, avenue Edouard Belin, F-31400 Toulouse, France

² Geneva Observatory, 51 Ch; des Maillettes, CH-1290 Versoix, Switzerland

³ Institute for Computational Cosmology, Department of Physics, University of Durham, DH1 3LE, UK

⁴ Laboratoire d'Astrophysique de Marseille, CNRS - Université Aix-Marseille, 38 rue Frédt'eric Joliot-Curie, 13388 Marseille Cedex 13, France

⁵ Steward Observatory, University of Arizona, 933 North Cherry Avenue, Tucson, AZ 85721, USA

2.2 Selection criteria

The spectral energy distribution (SED) of star-forming high- z galaxies is characterized by a strong break bluewards of Lyman-alpha and a blue continuum redwards. We used different filter combinations to identify galaxy samples fulfilling these criteria at different redshifts. In order to select sources at $z \geq 8$, we have imposed as detection criteria: $m_{H,K} \geq 5\sigma$ and $m_{I,z} \leq 2\sigma$. At redshift 7 these criteria become : $m_{Y,J} \geq 5\sigma$ and $m_I \leq 2\sigma$. According to the general considerations described above, the selection function is based on the position of galaxies on color-color diagrams defined from MC simulations and filter transmissions (Tab 1). Using these color selection, we have found 13 bright sources namely 1 J - drop, 8 Y -drops and 4 z -dropouts (some of them are shown on Fig 1). The magnitude in the H-band range between 23.35 and 26.51 and magnification factors are relatively modest (from 1.01 to 1.37).

	$z \geq 9$	$z \geq 8$	$z \geq 7$
Color Criteria	$J - H \geq 0.76$	$Y - J \geq 0.8$	$z - Y \geq 1.0$
	$H - K \leq 0.5$	$J - H \leq 1.2$	$Y - J \leq 1.2$
	$J - H \geq 1.3(H - K) + 0.76$	$Y - J \geq 1.25(J - H) + 0.8$	$z - Y \geq (Y - J) + 0.6$

Table 1. Color selection criteria adopted as a function of redshift

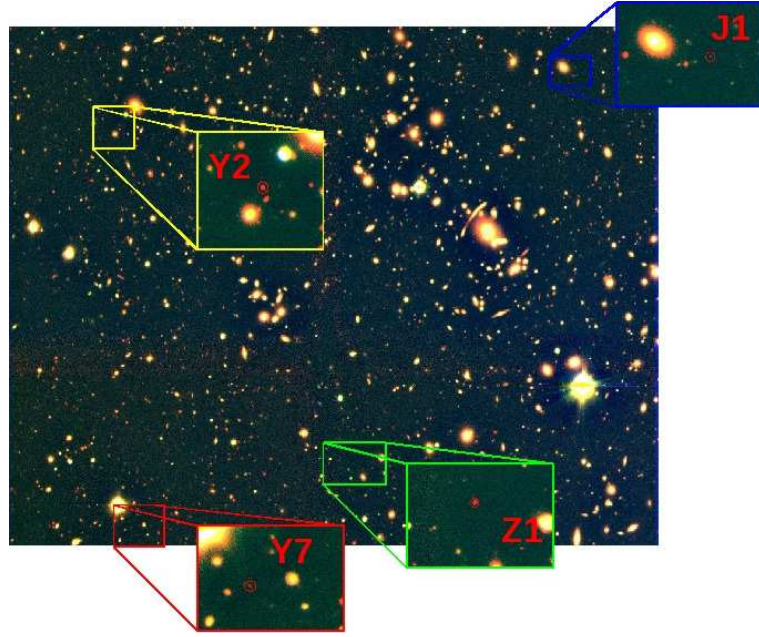


Fig. 1. Color image of Abell2667 including 4 sources from the high- z sample, presented in details in Laporte et al. (2011)

2.3 Contamination

Considering the evolving Luminosity Function (LF) from Bouwens et al. (2008), we expect to detect ~ 5 high- z sources in the field of A2667 in this range of magnitude, suggesting a strong contamination by low/mid- z interlopers. The SED-fitting work and photometric redshift including all optical and near IR data yield a best solution at high- z in all cases. When applying a luminosity prior and/or additional information (see below), only half of the sample survives. Indeed, a recent study of 2 sources from the sample (Boone et al. 2011) using submillimeter data from Herschel (instruments PACS and SPIRE) and LABOCA with wavelength ranging from 100 to $870\mu\text{m}$ has shown that standard templates from the literature fail to reproduce the visible photometry observed even if the far-IR/submillimeter data are correctly adjusted with ULIRGS or SMGs at $z \sim 2$. Due to the shape of their SED in optical and near-IR domain, these two objects appear as extreme sources which could contaminate other high- z samples.

3 Luminosity Functions

In this section we first present the main steps used to determine the LF. The results obtained at $z > 7$ will be presented together with a discussion on the evolution of the LF between $z \sim 7$ and 9

3.1 Method

We have used a method based on MC simulations to compute the LF following Bolzonella et al. (2002). This method is based on the probability distributions derived when computing photometric redshifts. Number densities were corrected from incompleteness as a function of magnitude and redshift, and error bars were derived according to Trenti & Stiavelli (2008) including cosmic variance and Poisson uncertainties.

The method includes the following steps: i) For each source and at each iteration, a probability a is randomly selected between 0 and 1; ii) According to the cumulated redshift probability distribution, a redshift z is attributed as follows $z \Rightarrow P(z) = a$; iii) The UV luminosity L_{1500} is derived as a function of redshift, taking into account the restframe SED and correcting for the magnification value; iv) The number of sources in each luminosity bin is determined, corrected for incompleteness, and finally translated into a number density using the corresponding (lensing corrected) covolume. The typical number of iterations is 1000 to derive a LF in a redshift bin.

3.2 Results

As explained above, we have found one J -dropout candidate (called J1 and presented in Fig 1) over our ~ 45 arcmin² field of view. This is one of the candidates for which a spectroscopic follow up is needed to conclude about its redshift and nature. For this reason, two cases have been considered: either J1 is a genuine high- z galaxy or it is a mid- z interloper instead (i.e. no J -dropout is found around A2667 up to the limits of this survey). In the former case, the number density is $\Phi(M = -21.5 \pm 0.5) = (6.76 \pm 5.0) \cdot 10^{-7} \text{Mpc}^{-3}$, which is consistent with upper limit from Bouwens et al. (2008) and points from Lorenzoni et al. (2010). In the later case, if no J -drop is found around A2667, we are able to give a strong constraint on the bright part of the LF considering a Poisson distribution. We found, at 68% confidence level, a limit of $\Phi(M = -21.5 \pm 0.5) \leq (5.17 \pm 5.0) \cdot 10^{-6} \text{Mpc}^{-3}$ which is also consistent with previous references (Fig 2 bottom left)

At $z \sim 8$, we have found 8 Y -dropouts with magnitude ranging between 23.35 and 25.40. We expect up to 75% contamination in this redshift bin. Waiting for additional (spectroscopic) data, we have performed different tests. The best results are obtained when applying a selection based on the optical χ^2 method following Bouwens et al. (2010). Two points are obtained with this new sub-sample: $\Phi(M = -22.0 \pm 0.25) = (0.18^{+2.8}_{-0.16}) \cdot 10^{-5} \text{Mpc}^{-3}$ and $\Phi(M = -21.5 \pm 0.25) = (0.12^{+1.5}_{-0.1}) \cdot 10^{-4} \text{Mpc}^{-3}$. These new results are consistent with McLure et al. (2010) and previous references (Fig 2 top right).

At lower redshift, $z \sim 7$, after removing Z1 from our sample based on its detection at 24 microns and the IR SED (see Boone et al. (2011)), we computed the LF from the 3 remaining objects and were able to give one point in the bright end of the LF : $\Phi(M = -21.25 \pm 0.25) = (8.5 \pm 7.6) \cdot 10^{-5} \text{Mpc}^{-3}$. This new result is consistent with results from Castellano et al. (2010) and Ouchi et al. (2009) (Fig 2 top left).

3.3 Evolution of the LF from $z \sim 7$ to 9

To study the evolution of the LF beyond $z \sim 7$, the usual parametrization based on the Schechter function (Schechter 1976) was used :

$$\Phi(M) = \Phi^* \frac{\ln(10)}{2.5} (10^{-0.4(M-M^*)})^{\alpha+1} \exp -10^{-0.4(M-M^*)} \quad (3.1)$$

A χ^2 minimization procedure was used to determine the best-fit LF parameters (namely Φ^* , M^* , and α), by combining our own results with those found by previous authors (see references in Sect. 3.2). Fig 2 displays three LFs (at $z \sim 7$, 8 and 9) together with the 68% likelihood contour from which error bars on each parameters are deduced. Tab. 2 summarizes these results as a function of redshift. Our observations cover the bright end of the LF and are therefore insensitive to the faint-end slope α . This value is assumed fixed at $z \sim 9$ for consistency, and the best-fit value at $z \sim 7$ and $z \sim 8$ is also consistent as expected with previous authors.

Given the error bars, the LF does not seem to evolve significantly between $z \sim 7$ and 8. This finding is consistent with results from Bouwens et al. (2010) who found no evidence of an evolution of the LF in this

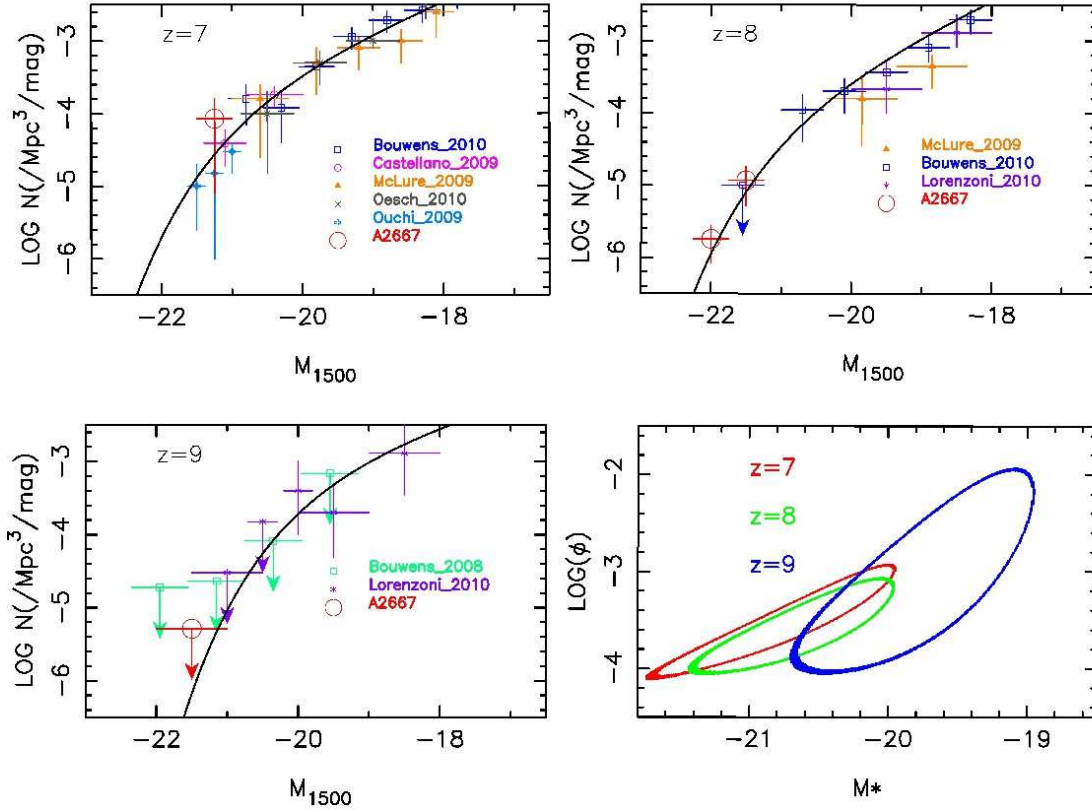


Fig. 2. LF at $z \sim 7$ (top-left), $z \sim 8$ (top-right) and $z \sim 9$ (bottom-left). Solid lines display the best-fit Schechter parametrization. At $z \sim 9$, the upper limit is shown. The 68% likelihood contours on the Schechter parameters are shown in the bottom-right panel

Redshift	M^*	Φ^* 10^{-3}Mpc^{-3}	α
$z \sim 7$	-20.53 ± 0.18	$0.40^{+0.4}_{-0.2}$	-2.00 ± 0.21
$z \sim 8$	-20.51 ± 0.35	$0.30^{+0.26}_{-0.14}$	-2.14 ± 0.20
$z \sim 9$	-19.52 ± 0.33	$1.37^{+1.7}_{-0.8}$	-1.74 (<i>fixed</i>)

Table 2. Parametrization of the LF using results from this work, together with Ouchi et al. (2009), Castellano et al. (2010), McLure et al. (2010), Bouwens et al. (2010), Lorenzoni et al. (2010), Bouwens et al. (2008)

redshift domain. A strong evolution between $z \sim 8$ and 9, with a sharp decrease in the number density of bright galaxies beyond $z \sim 8$, as expected by hierarchical models of galaxy formation.

4 Conclusions

The photometric survey conducted with HAWK-I and FORS2 on A2667 allowed us to identify a sample of 13 high- z candidates ($z \geq 6.5$) namely 1 J -drop, 8 Y -drops and 4 z -drops using a color selection based on the Lyman Break Technique (Laporte et al. 2011). This sample suffers from a relatively high contamination level from extreme mid- z interlopers, as demonstrated by the recent detection of two candidates by Herschel and LABOCA, making the high- z identification unlikely (Boone et al. 2011). Waiting for a complete spectroscopic follow up, we have used different criteria to account for this contamination and to derive new constraints on the bright end of the UV LF from $z \sim 7$ to 9, using a MC approach based on the redshift probability distributions. Our results are consistent with a significant evolution in the density of bright galaxies beyond $z \sim 8$, whereas no

clear evolution is observed between $z \sim 7$ and 8.

Part of this work was supported by the French Centre National de la Recherche Scientifique (CNRS), the French Programme National de Cosmologie et Galaxies (PNCG), as well as by the Swiss National Science Foundation. We acknowledge support for the International Team 181 from International Space Science Institute (ISSI) in Berne. This work received support from Agence Nationale de la Recherche (ANR) bearing the reference ANR-09-BLAN-0234. This paper is based on observations collected at the European Southern Observatory (ESO), Chile (71.A-0428,082.A-0163).

References

- Bolzonella, M., Pelló, R., & Maccagni, D. 2002, *A&A*, 395, 443
- Boone, F., Schaerer, D., Pello, R., et al. 2011, ArXiv e-prints : 1108.2406
- Bouwens, R. J., Illingworth, G. D., Franx, M., & Ford, H. 2008, *ApJ*, 686, 230
- Bouwens, R. J., Illingworth, G. D., González, V., et al. 2010, *ApJ*, 725, 1587
- Bouwens, R. J., Illingworth, G. D., Labbe, I., et al. 2011, *Nature*, 469, 504
- Castellano, M., Fontana, A., Paris, D., et al. 2010, *A&A*, 524, A28
- Laporte, N., Pelló, R., Schaerer, D., et al. 2011, *A&A*, 531, A74
- Lorenzoni, S., Bunker, A., Wilkins, S., et al. 2010, ArXiv e-prints
- McLure, R. J., Dunlop, J. S., Cirasuolo, M., et al. 2010, *MNRAS*, 403, 960
- Ouchi, M., Mobasher, B., Shimasaku, K., et al. 2009, *ApJ*, 706, 1136
- Richard, J., Kneib, J.-P., Ebeling, H., et al. 2011, *MNRAS*, 414, L31
- Schechter, P. 1976, *ApJ*, 203, 297
- Steidel, C. C., Pettini, M., & Hamilton, D. 1995, *AJ*, 110, 2519
- Trenti, M. & Stiavelli, M. 2008, *ApJ*, 676, 767
- Zwicky, F. 1937, *ApJ*, 86, 217